J Mater Sci (2016) 51:6411–6418

XPS study of the electronic density of states in the superconducting Mo_2B and Mo_2BC compounds

R. Escamilla[1,2,*], E. Carvajal[2], M. Cruz-Irisson[2], F. Morales[1], L. Huerta[1], and E. Verdin[3]

[1] *Instituto de Investigaciones en Materiales, Universidad Nacional Autónoma de México, Apartado Postal 70-360, 04510 Mexico, D.F., Mexico*

[2] *ESIME-Culhuacán, Instituto Politécnico Nacional, Av. Santa Ana 1000, CP 04430 Mexico, D.F., Mexico*

[3] *Departamento de Física, Universidad de Sonora, Apartado Postal 1626, CP 83000 Hermosillo, Sonora, Mexico*

Received: 27 January 2016
Accepted: 28 March 2016
Published online: 5 April 2016

ABSTRACT

The electronic structure of the Mo_2BC and Mo_2B compounds was investigated by X-ray photoelectron spectroscopy. The Mo 3d, C 1s, and B 1s core levels are identified. For the Mo_2BC, the core-level binding energies corresponding to Mo $3d_{5/2}$, B 1s, and C 1s are localized at 227.90, 187.94, and 282.95 eV, respectively, whereas for the Mo_2B, the Mo $3d_{5/2}$, and B 1s are localized at 228.09 and 188.06 eV, respectively. Core-level binding energies shifts are observed in both compounds using the charge-potential model. The electronic density of states was calculated for Mo_2B and Mo_2BC using GGA approximation. Our results show that the electronic density of states at the Fermi level in the Mo_2B is higher than that in the Mo_2BC. The dominance of the Mo 4d states down to 8 eV below the Fermi level is found. The calculated total DOS was consistent with the XPS valence band spectra. Finally, within the BCS theory framework, the presence of superconductivity in both compounds can not be explained only as a function of the electronic density of states at the Fermi level. The electron-phonon coupling constant (λ) was calculated using the McMillan equation; the obtained values were 0.75 for Mo_2BC and 0.70 for Mo_2B. These values indicate that both compounds are intermediate coupled superconductors.

Introduction

The discovery of superconductivity in MgB_2 at 40 K by Nagamatsu et al. [1] has renewed a great interest in the boron compounds; for example, borides, diborides, hexaborides, and dodecaborides [2]. From these compounds, the Mo-based ones are interesting because some are superconductors. The dimolybdenum boride Mo_2B (Al_2Cu-type structure) shows a body-centered tetragonal structure (space group I4/mcm) with $Z = 4$. The Wyckoff positions are Mo: 8h (0.17, 0.67, 0) and B: 4a (0, 0, 0.25), the corresponding site point group is 422. Each B atom has eight nearest Mo atoms. The coordinate number of Mo atom is 15, with four Mo–B bonds [3]. However, recently it has been reported that the Mo_2B tetragonal structure with space group I4/

Address correspondence to E-mail: rauleg@unam.mx

DOI 10.1007/s10853-016-9938-z

mcm is dynamically unstable at ambient pressure respect to the tetragonal structure with space group I4/m and Wyckoff positions Mo: 8h (0.1626, 0.6770, 0.0000) and B: 4e (0.0000, 0.0000, 0.2871)[4]. When C atoms are introduced into the structure of Mo_2B, the borocarbide molybdenum Mo_2BC is formed; it crystallizes in a face-centered orthorhombic structure (space groupe Cmcm). The C atoms are located at the center of [Mo_6C] distorted octahedra, which share edges to form layers and B atoms forming zigzag chains passing through the centers of trigonal prisms of Mo atoms [5].

The Mo_2BC and Mo_2B compounds are superconductors with critical temperature (T_c) ~7.5 K [6] and ~5.8 K [7], respectively. In these compounds, the mechanism of superconductivity may be similar to the observed in nonstoichiometric compounds such as $MoB_{2.5}$, $NbB_{2.5}$, and others [8–11]. Details of the electronic structure have been reported for Mo_2B and Mo_2BC compounds [4, 12–14]. However, until now the role of the chemical shifts via the core-level binding energies and the contribution of Mo 4d, B 2p, and C 2p orbitals to the electronic density of states (DOS) have not been carried out in these compounds. Therefore, in the present work we report the electronic structure studies by X-ray photoemission spectroscopy (XPS) and calculations of the partial and total electronic density of states. In addition, the electron-phonon coupling constant was determined and indicates that both compounds are intermediate coupling superconductors.

Experimental and calculation details

Polycrystalline sample of Mo_2BC was synthesized by the arc-melting method using Mo_2B (Aldrich, powder <325 mesh) and carbon (99.5 % powder, crystalline, <57 mesh, 99.5 mass %), as precursors. They were mixed in stoichiometric amounts and pressed into a pellet of 13 mm in diameter and 0.5 g in weight. Mo_2BC and Mo_2B pellets were melted and solidified on a water-cooled copper hearth in an Ar (99.999%) atmosphere. The X-ray diffraction patterns were recorder in a Bruker axs D8 Advance diffractometer using Cu Kα radiation with a Ni filter. The counts were collected in steps of 0.02° for 14 s in the 2θ range 10°–120° at room temperature. The lattice parameters were refined using the Rietveld program, based on the least-squares method [15]. DC magnetization measurements as a function of temperature, $M(T)$, were performed in a Quantum Design SQUID-based magnetometer at temperatures from 2 to 10 K with an external magnetic field of 10 Oe. The electronic structure and the chemical analysis were carried out by X-ray photoelectron spectroscopy (XPS) using a UHV system of VG Microtech ESCA2000 Multilab, with an Al K X-ray source ($h\nu$ = 1486.6 eV), and CLAM4 MCD analyzer. The surface of polycrystalline samples was etched for 10 min with Ar^+ ions produced with 4.5 kV at 0.33 μA mm^{-2}. The XPS spectra were obtained at 55° from the normal to the surface in the constant pass energy mode (CAE), E_0 = 50 and 20 eV for surface and high-resolution narrow scan, respectively. The peak positions were referenced to the C 1s core-level of the hydrocarbon groups localized at 285.00 eV. The XPS spectra were fitted using the SDP v 4.1 program [16]. The XPS error was estimated in deconvolution analyzes error at 5 % (i.e. ±0.05 eV).

The first-principles calculations were performed with the CASTEP code [17, 18] based on density functional theory (DFT) [19, 20]. The correlation functional was treated by the generalized gradient approximation (GGA), as proposed by Perdew–Wang (PW91) [21]. The tightly bound core electrons were represented by nonlocal ultra-soft pseudo-potentials of the Vanderbilt-type [22]. The two parameters that affect the accuracy of calculations are the kinetic energy cut-off and the number of k-points used for the Brillouin zone [23]. The kinetic energy cut-off used for the Brillouin zone was 500 eV and a $11 \times 11 \times 11$ k-points mesh. The convergence tolerances were set as follows: 0.002 eV/Å for the maximum force on atoms, 10^{-4} Å for the maximum atomic displacement, and 0.003 GPa for the highest strain amplitude.

Results and discussion

X-ray diffraction patterns for Mo_2BC and Mo_2B polycrystalline samples are shown in Fig.1a, b, respectively. The X-ray diffraction patterns were identified as Mo_2BC (ICSD No 29-0913) and Mo_2B (ICSD No 01-073-1766). Faint features of the Mo_2C phase (ICDD No 35-0787) were observed in the Mo_2BC sample. The calculated lattice parameter for Mo_2BC with an orthorhombic structure and space group Cmcm (No. 63) were a = 3.0862(3) Å, b =

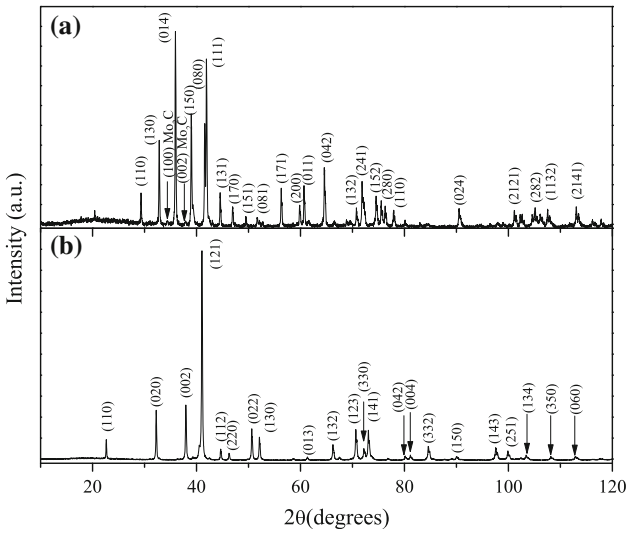

Figure 1 X-ray diffraction patterns for the **a** Mo_2BC and **b** Mo_2B polycrystalline samples.

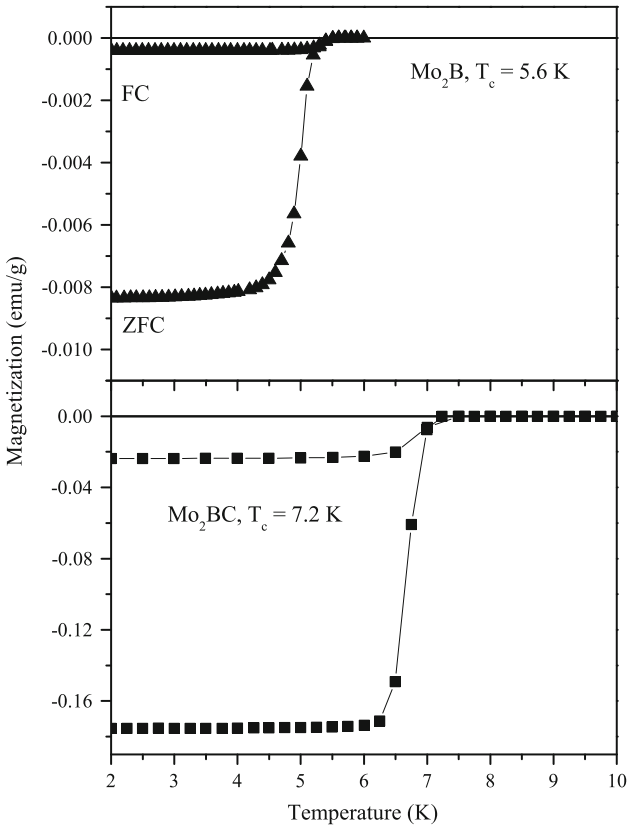

Figure 2 Susceptibility versus temperature curves of the Mo_2BC and Mo_2B samples.

17.3434(3) Å and c = 3.0472(2) Å; while for Mo_2B with a tetragonal structure and space group I4/m (No. 87) were a = 5.5469(3) Å and c = 4.7383(3) Å. The calculated lattice parameters are in agreement with those reported previously for Mo_2B [3] and Mo_2BC [5].

Figure 2 shows the temperature dependence of DC-magnetization $M(T)$ measured from 10 K to 2 K in an applied field of 10 Oe. The measurements were performed in the zero field cooled (ZFC) and field cooled (ZF) conditions. The superconducting transition temperature T_c was defined by the onset of the diamagnetic signal. T_c of about 7.2 and 5.6 K were determined for Mo_2BC and Mo_2B, respectively. These values are in agreement with those reported previously, for Mo_2BC [6] and for Mo_2B [7]. The amount of superconducting phase was estimated at 12 and 5 % for Mo_2BC and Mo_2B, respectively. It is pointed out that the amount of superconducting phase determination is ambiguous because the presence of flux-pinning underestimates it [24]. It is noteworthy that in the MT) curve of Mo_2BC there is not a signal of the Mo_2C transition (T_c = 3.6 K) [25], despite Mo_2C traces observed in the X-ray diffraction pattern.

The core-level binding energy (CLBE) of the chemical components of Mo_2B and Mo_2BC was determined by XPS measurements. Figure 3 shows the XPS survey spectrum of the samples after Ar^+ ion etching. The spectra show the Mo 3p, Mo 3d, C 1s, and B 1s core levels.

The high-resolution XPS spectra of Mo 3d and B 1s core levels for the Mo_2BC and Mo_2B compounds are shown in Fig.4. In this figure, it is observed that B 1s and Mo 3d core-level intensity is similar to both compounds. The Mo $3d_{5/2}$ CLBE is localized at 227.79 eV (Fig. 4a) and 228.09 eV (Fig. 4b) in Mo_2BC and Mo_2B, respectively. Similar results were found for carbides [26] and borides [26, 27] based on molybdenum. Additionally, the deconvolution of the Mo $3d_{5/2}$ and Mo $3d_{3/2}$ spectra show a small contribution at 229.16 and 232.30 eV in both compounds, which are associated with MoO_2 [28]. In Fig. 4c, d is shown the B 1s core-level of Mo_2BC and Mo_2B, respectively. The signal intensity is low; however, it was possible to resolve the binding energy in both samples. The B 1s CLBE was located at 187.94 eV in Mo_2BC and at 188.06 eV in Mo_2B. These CLBE values are in agreement with those reported previously in transition metal borides [27, 29], diborides [26, 27, 30], and borocarbides [31].

The Mo_2BC XPS survey spectrum shows the C 1s core-level, the high-resolution spectrum is shown in Fig. 5. The signal is fitted assuming two components; the first one located at 282.95 eV corresponds to

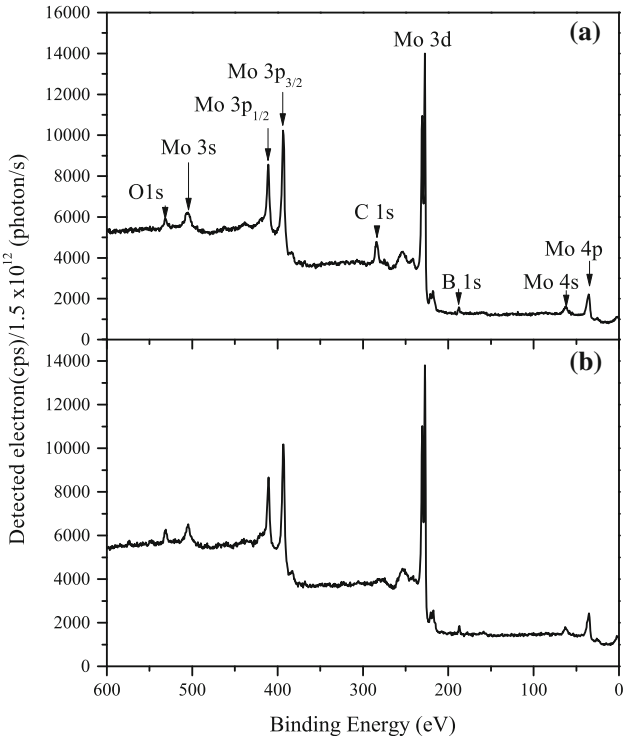

Figure 3 XPS survey spectrum after Ar^+ etching for the **a** Mo_2BC and **b** Mo_2B samples.

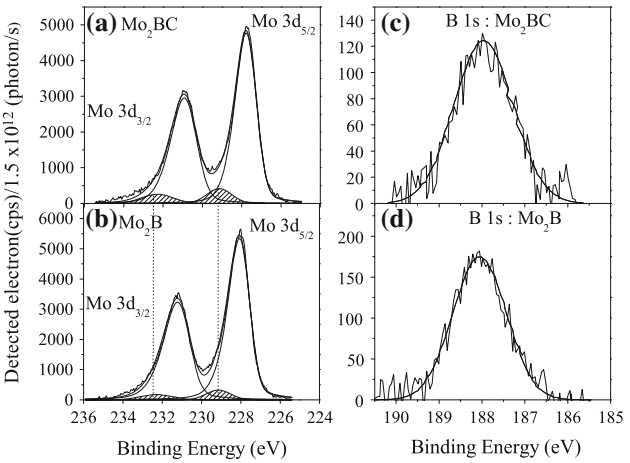

Figure 4 High-resolution XPS spectra of the Mo 3d for **a** Mo_2BC and **b** Mo_2B samples. High-resolution XPS spectra of the B 1s for **c** Mo_2BC and **d** Mo_2B samples. The *shaded area* in the Mo 3d panel corresponds to MoO_2.

Mo_2BC, characteristic of borocarbides [31] and transition-metal carbides [26, 32–35]. The second one localized at 285.00 eV that corresponds to C non-reacted.

The charge-potential model has been proposed to explain the CLBE shift in compounds and disordered

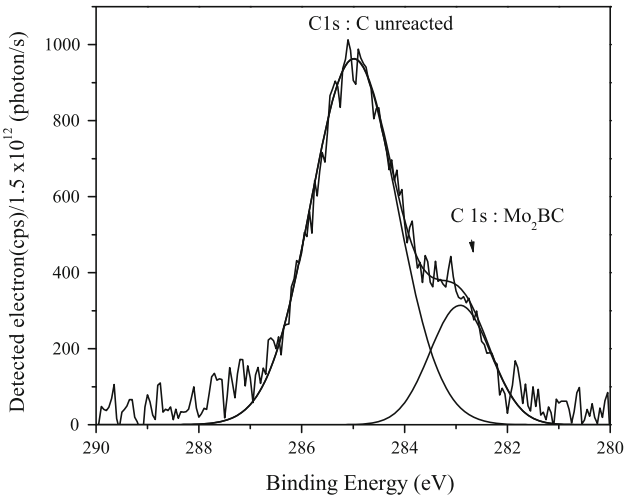

Figure 5 High-resolution XPS spectra of the C 1s, core-level for the Mo_2BC sample.

Table 1 Core-level binding energies for Mo_2BC, Mo_2B and reference materials

Sample	Mo $3d_{5/2}$	B 1s	C 1s
Mo_2BC	227.79	187.94	282.95
Mo_2B	228.09	188.06	
Mo	227.90		
B		187.30	
C			285.00

All values are in eV

alloys under the assumption that the final state effects and volume change are negligible [36]. In this interpretation, the general rule is that the binding energy of the central atom increases as the electronegativity of the attached atoms or groups increases. According to Pauling's electronegativity table [37], the Mo (2.16) is more electronegative than B (2.04) but is less electronegative than C (2.55). It is expected that the C core-level shifts toward lower binding energies and the Mo and B core-level shift toward higher binding energies.

The CLBE shifts are observed in the binary transition-metal carbides MC (M = 3d transition-metal) [32, 35] indicating that some charge transfer occurred from M atoms to carbon atoms. The analysis of Mo $3d_{5/2}$, B 1s and C 1s CLBE of Mo_2BC and Mo_2B spectra shows the core-level energy shift (ΔMo $3d_{5/2}$, ΔB 1s and ΔC 1s). Table 1 shows the core-level binding energies and Table 2 shows the chemical shift (Δ) for Mo_2BC, Mo_2B and reference material, respectively. From the data in

Table 2 Chemical shift (Δ) for Mo_2BC and Mo_2B

Sample	ΔMo 3d $_{5/2}$	ΔB 1s	ΔC 1s
Mo_2BC	0.11	−0.64	2.05
Mo_2B	−0.19	−0.76	

All values are in eV

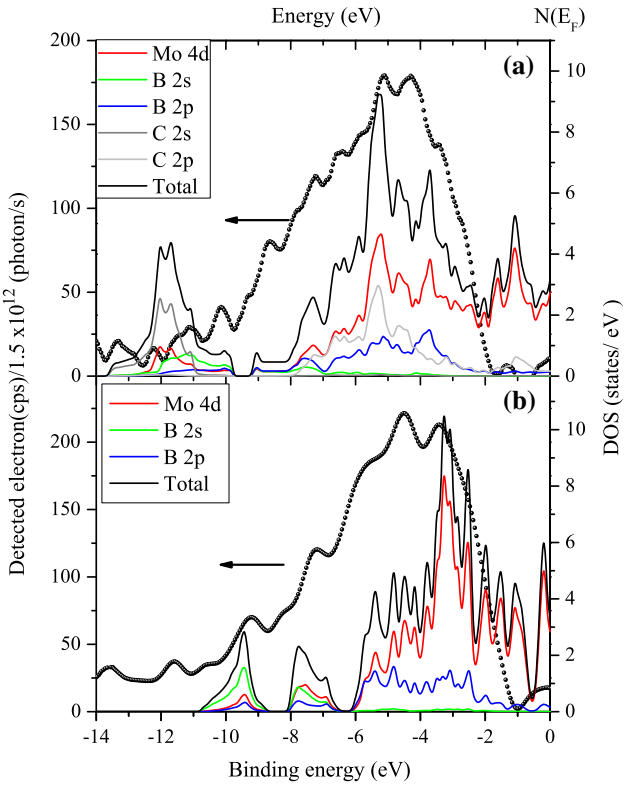

Figure 6 Valence band (*dots*) determined by XPS measurements and electronic density of states (*continuous lines*) calculated for Mo_2BC (**a**) and Mo_2B (**b**). Calculations include the partial and total density of states (scale on the *right side* correspond to DOS and the *left side* to XPS valence band).

Table 2, it is possible to see that the general rule, based on the electronegativity, is applicable to the Mo_2BC and Mo_2B compounds. Similar results were reported for TaC [32] and MgB_2 [38].

Additional information can be extracted from the XPS measurements. Figure 6 shows the XPS valence band spectra and the total and partial electronic density of states (DOS) calculated for Mo_2BC and Mo_2B compounds. The DOS of Mo_2BC and Mo_2B was calculated from first-principles using the CASTEP code [17, 18]. The results show that the electronic density of states at the Fermi level $N(E_F)$ for Mo_2BC (3.06 states/eV) is lower than the corresponding to Mo_2B (3.42 states/eV). The $N(E_F)$ is in agreement with those reported previously for Mo_2B [4] and Mo_2BC [14]. A good concordance between XPS valence band and DOS is observed in Mo_2BC; however in the Mo_2B, a shift to higher binding energy of the DOS respect to XPS valence band is observed. This shift is not a generalized behavior as seen in Mo_2BC and other compounds [39, 40]. However, in high-temperature superconductors, a good correspondence can be obtained if the DOS is shifted around 2 eV to higher binding energy; this difference is usually due to electron correlation effects [41, 42]. In this work, the electron correlation effects are not considered.

For Mo_2BC, the contributions to total DOS between −10.5 and −12.5 eV are from the non-bonding B 2s and C 2s states, meanwhile the feature between −3.0 and −8.0 eV is due to the hybridization between Mo 4d, C 2p, and B 2p states [14]. The Mo 4d–B 2p hybridized states are lower in energy than the Mo 4d–C 2p hybridized states ones, suggesting that Mo–C bonds are stronger than Mo–B bonds. For Mo_2B, the B 2s and B 2p states are localized from −6.0 to −10.0 eV and from −6.0 up to −1.0 eV, respectively. The feature from −1.0 and −6.0 eV is due to covalent hybridization between Mo 4d–B 2p bonding states [4]. Finally, near the Fermi level, the calculated DOS is formed mainly by Mo 4d states.

XPS measurements on polycrystalline samples provide the same information of the core-level spectrum and valence band than XPS measurements on thin films and single-crystals surfaces, as previous reports have been shown [42, 43].

It is noteworthy that the $N(E_F)$ of Mo_2BC is lower than $N(E_F)$ of Mo_2B, but, T_c of Mo_2BC is higher than the T_c of Mo_2B. From the view point of the BCS theory $N(E_F)$ and T_c are related by the following expression [44]:

$$T_c = 1.14\theta_D \exp\left[\frac{-1}{N(E_F)V}\right], \quad (1)$$

where θ_D is the Debye temperature, $N(E_F)$ is the electronic density of states at Fermi level, and V is related to the electron-phonon interaction. According to this expression, large values of $N(E_F)$ and/or electron-phonon interaction lead to high T_c values. This fact indicates that for these compounds $N(E_F)$ plays a second role in the effect of $N(E_F)$ on T_c. Thus, the electron-phonon interaction might play a preponderant role in the origin of superconductivity in these compounds. For example, the high T_c in the

Table 3 Superconducting critical temperature (T_c), Debye temperature (θ_D), electronic density of states at Fermi level $N(E_F)$ and electron-phonon coupling constant (λ) for Mo_2BC and Mo_2B

Sample	T_c (K)	θ_D (K)	$N(E_F)$ (states/eV)	λ
Mo_2BC	7.2	529 [50]	3.06	0.75
Mo_2B	5.6	364 [51]	3.42	0.70

transition metal carbides and nitrates results primarily from the relatively large values of λ [45], differing of A15 compounds which their high T_c results from large $N(E_F)$ values [46, 47]. However, there is no consensus about the relation between Debye temperature θ_D and T_c. For example, in high-T_c oxide superconductors, Abd-Shukor [48] suggests that θ_D does not correlate with T_c while that Ledbetter [49] proposes that if there is such a relationship. Moreover, Ledbetter [49] suggests that in BCS materials, T_c increases with decreasing θ_D. This behavior is not observed in our results (see Table 3).

According to the BCS theory, the electron-phonon coupling constant can be determined using the semiempirical formula of McMillan [52], expressed as

$$T_c = \frac{\theta_D}{1.45}\exp\left[\frac{-1.04(1+\lambda)}{\lambda-\mu^*(1+0.62\lambda)}\right], \quad (2)$$

where μ^* is the Coulomb pseudopotential that is related to the screened Coulomb interaction, and λ is the electron–phonon coupling constant. Using Eq. (2) and $\mu^* = 0.13$, we obtain $\lambda = 0.75$ for Mo_2BC and 0.70 for the Mo_2B compound. The electron-phonon coupling constant is similar to both compounds, and the values obtained indicate that Mo_2BC and Mo_2B are intermediate coupled superconductors. Table 3 summarizes the parameter's values used to calculate λ. As a conclusion, the phonon density of states is more important than $N(E_F)$ in Mo_2BC and Mo_2B, as can be inferred from Eq. (1) and the corresponding values of θ_D. Experimental and calculations of the phonon density of states are required to determine the differences between the phonon modes involved in the superconducting state of the Mo_2BC and Mo_2B compounds.

Conclusions

The Mo_2BC polycrystalline sample was synthesized by the arc-melting method from commercially available Mo_2B powder precursor. X-ray diffraction studies showed that the compounds are mainly single phase. Magnetization measurements revealed that the Mo_2BC and Mo_2B have T_c values of 7.2 and 5.6 K, respectively. Comparing the core-level binding energies of both compounds with the Mo metal, B crystalline, and C, we observed chemical shifts most probably due to the mechanism of charge transfer. The XPS valence band measurements of Mo_2BC and Mo_2B compounds were consistent with the total DOS. The significant contribution to the electronic density of states at the Fermi level, in both compounds, is from Mo 4d states which are the main responsible of the metallic behavior. The electron-phonon coupling constant of both compounds indicates that they are intermediate coupled superconductors and that the phonon density of states plays a major role than $N(E_F)$ on the superconducting temperature.

Acknowledgements

The authors thank the Projects DGAPA-UNAM IN-106116, SIP-20141640 and SIP-20141641 from IPN. Financial support to PASPA-DGAPA and also, for their technical help to F. Silvar, M.M.S. Alberto Lopez-Vivas, J. Morales and C. González. Calculations were done using resources from the Supercomputing Center DGTIC-UNAM.

References

[1] Nagamatsu J, Nakagawa N, Muranaka T, Zenitani Y, Akimitsu JJ (2001) Superconductivity at 39 K in magnesium diboride. Nature 410:63–64

[2] Buzea C, Yamashita T (2001) Review of the superconducting properties of MgB_2. Supercond Sci Technol 14:R115–R146

[3] Kiessling R (1947) The crystal structures of molybdenum and tungsten borides. Acta Chem Scand 1:893–916

[4] Zhou D, Wang J, Cui Q, Li Q (2014) Crystal structure and physical properties of Mo_2B: first-principle calculations. J Appl Phys 115:113504

[5] Jeitschko W, Nowotny H, Benesovsky F (1963) Die Kristallstruktur von Mo_2BC. Monatsh Chem 94:565–568

[6] Lejay P, Chevalier B, Etourneau J, Hagenmuller P (1981) Influence of some metal substitutions on the superconducting behaviour of molybdenum borocarbide. J Less Common Met 82:193–200

[7] Engelhardt JJ (1969) Superconducting isotope effect in molybdenum boride and tungsten boride. Phys Rev 179:452–458

[8] Fisk Z (1991) Superconducting borides. AIP Conf Proc 231:155–164
[9] Yamamoto A, Takao C, Masui T, Izumi M, Tajima S (2002) High-pressure synthesis of superconducting $Nb_{1-x}B_2$ (x = 0–0.48) with the maximum T_c = 9.2 K. Phys C 383:197–206
[10] Escamilla R, Lovera O, Akachi T, Duran A, Falconi R, Morales F, Escudero R (2004) Crystalline structure and the superconducting properties of NbB_{2+x}. J Phys 16:5979–5990
[11] Young DP, Goodrich RG, Adams PW, Chan JY, Fronczek FR, Drymiotis F, Henry LL (2002) Superconducting properties of $BeB_{2.75}$. Phys Rev B 65:80518(R)
[12] Bolvardi HI, Emmerlich J, Baben M, Music D, von Appen J, Dronskowski R, Schneider JM (2013) ystematic study on the electronic structure and mechanical properties of X2BC (X = Mo, Ti, V, Zr, Nb, Hf, Ta and W). J Phys 25:045501
[13] Emmerlich J, Music D, Braun M, Fayek P, Munnik F, Schneider JM (2009) A proposal for an unusually stiff and moderately ductile hard coating material: Mo_2BC. J Phys D 42:185406
[14] Falconi R, de la Mora P, Morales F, Escamilla R, Camacho CO, Acosta M, Escudero R (2015) High-pressure and electronic band structure studies on Mo_2BC. J Low Temp Phys 179:158–165
[15] Altomare A, Burla MC, Giacovazzo C, Guagliardi A, Moliterni AG, Polidori G, Rizzi R (2001) Quanto: a Rietveld program for quantitative phase analysis of polycrystalline mixtures. J Appl Crystallogr 34:392–397
[16] 2004 SDP v4.1 (32 bit) Copyright XPS International, LLC, Compiled 17 January (2004)
[17] Payne MC, Teter MP, Allan DC, Arias TA, Joannopoulos JD (1992) Iterative minimization techniques for ab initio total-energy calculations: molecular dynamics and conjugate gradients Rev. Mod Phys 64:1045–1097
[18] Segall MD, Lindan PJD, Probert MJ, Pickard CJ, Hasnip PJ, Clark SJ, Payne MC (2002) First-principles simulation: ideas, illustrations and the CASTEP code. J Phys 14:2717–2744
[19] Hohenberg P, Kohn W (1964) Inhomogeneous electron gas. Phys Rev 136:B864–B871
[20] Kohn W, Sham LJ (1965) Self-consistent equations including exchange and correlation effects. Phys Rev 140:A1133–A1138
[21] Perdew JP, Wang Y (1992) Accurate and simple analytic representation of the electron-gas correlation energy. Phys Rev B 45:13244–13249
[22] Vanderbilt D (1990) Soft self-consistent pseudopotentials in a generalized eigenvalue formalism. Phys Rev B 41:7892–7895
[23] Monkhorst HJ, Pack JD (1976) Special points for Brillouin-zone integrations. Phys Rev B 13:5188–5192
[24] Radaelli PG, Hinks DG, Mitchell AW, Hunter BA, Wagner JL, Dabrowski B, Vandervoort KG, Viswanathan HK, Jorgensen JD (1994) Structural and superconducting properties of $La_{2-x}Sr_xCuO_4$ as a function of Sr content. Phys Rev B 49:4163–4172
[25] Xu C, Wang L, Liu Z, Chen L, Guo J, Kang N, Ma X-L, Cheng H-M, Ren W (2015) Large-area high-quality 2D ultrathin Mo_2C superconducting crystals. Nat Mater 14:1135–1141
[26] Brainard WA, Wheeler DR (1978) An XPS study of the adherence of refractory carbide silicide and boride rf-sputtered wear-resistant coatings. J Vac Sci Technol 15:1801
[27] Mavel G, Escard J, Costa P, Castaing J (1973) ESCA surface study of metal borides. Surf Sci 35:109–116
[28] Sarma DD, Rao CNR (1980) XPES studies of oxides of second- and third-row transition metals including rare earths. J Electron Spectrosc Relat Phenom 20:25–45
[29] Joyner DJ, Johnson O, Hercules DM (1970) A study of the iron borides. Electron spectroscopy. J Am Chem Soc 102:1910–1917
[30] Escamilla R, Huerta L (2006) X-ray photoelectron spectroscopy studies of non-stoichiometric superconducting NbB_{2+x}. Supercond Sci Technol 19:623–628
[31] Kobayashi K, Mizokawa T, Mamiy K, Sekiyama A, Fujimori A, Takagi H, Eisaki H, Uchida S, Cava RJ, Krajewski JJ, Peck WF Jr. (1996) Photoemission study of Ni borocarbides: superconducting YNi_2B_2C and nonsuperconducting $LaNi_2B_2C$. Phys Rev B 54:507–514
[32] Khyzhu OY (1999) Electronic structure and charge state of atoms of cubic and hexagonal tantalum carbides. Powder Metall Met Ceram 38:284–291
[33] Magnuson M, Lewin E, Hultman L, Jansson U (2009) Electronic structure and chemical bonding of nanocrystalline-TiC/amorphous- C nanocomposites. Phys Rev B 80:235108
[34] Furlan A, Lu J, Hultman L, Jansson U, Magnuson M (2014) Crystallization characteristics and chemical bonding properties of nickel carbide thin film nanocomposites. J Phys 26:415501
[35] Dai-Yi Q, Zi G (1990) XPS study of tungsten carbide Chin. J Chem 8:301–305
[36] Siegbahn K, Nordling C, Johansson G, Hedman J, Hedn PF, Hamrin K, Gelius U, Bergmark T, Werme LO, Manne R, Baer Y (1969) ESCA applied to free molecules. North-Holland, Amsterdam
[37] Pauling L (1957) The nature of the chemical bond, 3rd edn. Cornell University Press, Ithaca
[38] Talapatra A, Bandyopadhyay SK, Sen P, Barat B, Mukherjee S, Mukherjee M (2005) X-ray photoelectron spectroscopy

studies of MgB_2 for valence state of Mg. Phys C 419:141–147

[39] Kurmaev EZ, McLeod JA, Buling A, Skorikov NA, Moewes A, Neumann M, Korotin MA, Izyumov YA, Ni N, Canfield PC (2009) Contribution of Fe 3d states to the Fermi level of $CaFe_2As_2$. Phys Rev B 80:054508

[40] Gamza M, Slebarski A, Deniszczyk J (2006) Electronic structure of $CeRhIn_5$ and $CeIrIn_5$. Mater Sci Pol 24:569–577

[41] Likhachev ER, Dubrovskii OI, Kurganskii SI, Domashevskaya EP (1998) Analysis of photoelectron spectra of high-temperature superconductors. J Electron Spectrosc Relat Phenom 88–91:479–483

[42] Vasquez RP, Jung CU, Park MS, Kim HJ, Kim JY, Lee SI (2001) X-ray photoemission study of MgB_2. Phys Rev B 64:052510

[43] Shen ZX, Lindberg PAP, Wells BO, Mitzi DB, Lindau I, Spicer WE, Kapitulnik A (1988) Valence-band and core-level photoemission study of single-crystal $Bi_2CaSr_2Cu_2O_8$ superconductors. Phys Rev B 38:11820–11823

[44] Bardeen J, Cooper LN, Schrieffer JR (1957) Theory of superconductivity. Phys Rev 108:1175–1204

[45] Isaev EI, Ahuja R, Simak SI, Lichtenstein AI, Vekilov YK, Johansson B, Abrikosov IA (2005) Anomalously enhanced superconductivity and ab initio lattice dynamics in transition metal carbides and nitrides. Phys Rev B 72:064515

[46] Junod A, Jarlborg T, Muller J (1983) Heat-capacity analysis of a large number of A15-type compounds. Phys Rev B 27:1568–1585

[47] Paduani C (2007) Electronic Structure of the A3B Compounds: A = Nb; B = Al, Ga, Ge, Sn and In. Braz J Phys 37:1073–1076

[48] Abd-Shukor R (2007) Electron-phonon coupling constant of cuprate based high temperature superconductors. Solid State Commun 142:587–590

[49] Ledbetter H (1994) Dependence of T_c on Debye temperature θ_D for various cuprates. Phys C 235–240:1325–1326

[50] Toth LE, Zbasnik J, Sato Y, Gardner W (1968) Anisotropy in single-crystal refractory compounds. Plenum Press, New York, p 249

[51] Blinder AV, Bolgar AS (1991) Heat capacity and enthalpy of transition-metal borides in a broad range of temperatures Soviet. Powder Metall Met Ceram 30:1053–1056

[52] McMillan WL (1968) Transition temperature of strong-coupled superconductors. Phys Rev 167:331–344